# Identifying Human Parieto-Insular Vestibular Cortex Using fMRI and Cytoarchitectonic Mapping

**Simon B. Eickhoff,[1–3]* Peter H. Weiss,[1,3,4] Katrin Amunts,[1,3,5] Gereon R. Fink,[1,3,4] and Karl Zilles[1–3]**

[1]*Institut für Medizin, Forschungszentrum Jülich, Jülich, Germany*
[2]*C. & O. Vogt Institut für Hirnforschung, Düsseldorf, Germany*
[3]*Brain Imaging Centre West, Forschungszentrum Jülich, Jülich, Germany*
[4]*Neurologische Klinik, Universitätsklinikum Aachen, Aachen, Germany*
[5]*Klinik für Psychiatrie und Psychotherapie, Universitätsklinikum Aachen, Aachen, Germany*

**Abstract:** The parieto-insular vestibular cortex (PIVC) plays a central role in the cortical vestibular network. Although this region was first defined and subsequently extensively studied in nonhuman primates, there is also ample evidence for a human analogue in the posterior parietal operculum. In this study, we functionally and anatomically characterize the putative human equivalent to macaque area PIVC by combining functional magnetic resonance imaging (fMRI) of the cortical response to galvanic vestibular stimulation (GVS) with probabilistic cytoarchitectonic maps of the human parietal operculum. Our fMRI data revealed a bilateral cortical response to GVS in posterior parieto-insular cortex. Based on the topographic similarity of these activations to primate area PIVC, we suggest that they constitute the functionally defined human equivalent to macaque area PIVC. The locations of these activations were then compared to the probabilistic cytoarchitectonic maps of the parietal operculum (Eickhoff et al. [2005a]: Cereb Cortex, in press; Eickhoff et al. [2005c]: Cereb Cortex, in press), whereby the functionally defined PIVC matched most closely the cytoarchitectonically defined area OP 2. This activation of OP 2 by vestibular stimulation and its cytoarchitectonic features, which are similar to other primary sensory areas, suggest that area OP 2 constitutes the human equivalent of macaque area PIVC. *Hum Brain Mapp 27:611–621, 2006.* © 2005 Wiley-Liss, Inc.

**Key words:** hemispheric dominance; BOLD; galvanic stimulation; anatomy; operculum; insular cortex

## INTRODUCTION

To increase our knowledge of the neuronal underpinnings of vestibular information processing in the human central nervous system (CNS) is important, as the vestibular system plays a key role in motion perception, eye movements, and posture control [reviewed in Berthoz, 1996]. Many of these complex functions require an integrated processing of vestibular, visual, and somatosensory information about the position of our eyes, head, and body relative to the external world, thus operating in both ego- and allocentric frames of reference [for a review see Vogeley and Fink, 2003]. These processes rely on both cortical and subcortical structures. For example, extensive processing of vestibular afferents at the subcortical level, in particular in the brainstem and the cerebellum, is important for gaze control and postural stability. In contrast, orientation in space and the perception of movement also require considerable amount of processing of vestibular information at the cortical level. Consequently, several multimodal sensory areas integrating vestibular, visual, and somatosensory signals have been described in the cerebral cortex of nonhuman primates [Fredrickson et al., 1966; Guldin and Grusser, 1998; Ödkvist et al., 1973].

Contract grant sponsor: National Institute of Mental Health; Contract grant sponsor: National Institute of Neurological Disorders and Stroke; Contract grant sponsor: National Institute of Drug Abuse; Contract grant sponsor: National Cancer Centre; Contract grant sponsor: Deutsche Forschungsgemeinschaft; Contract grant number: KFO-112.

*Correspondence to: Simon B. Eickhoff, Institut für Medizin, Forschungszentrum Jülich GmbH, D-52425 Jülich, Germany.
E-mail: S.Eickhoff@fz-juelich.de

Received for publication 29 March 2005; Accepted 22 July 2005
DOI: 10.1002/hbm.20205
Published online 9 November 2005 in Wiley InterScience (www.interscience.wiley.com).

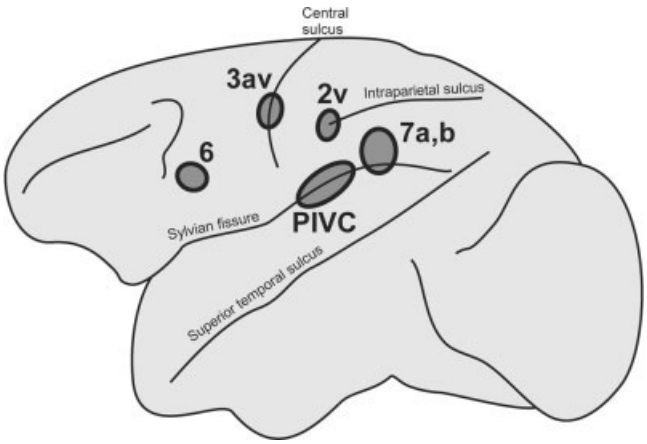


**Figure 1.**
Schematic drawing of the monkey brain, showing the location of vestibular areas in nonhuman primates. The areas that have been shown to receive vestibular input are area 2v at the tip of the intraparietal sulcus, area 3av in the central sulcus (i.e., the neck representation in somatosensory area 3a), areas 7a and 7b in the inferior parietal lobe, precentral area 6, and the parieto-insular vestibular cortex (PIVC) in the posterior parietal operculum in the depth of the Sylvian fissure.

Subsequently, a set of cortical areas has been identified in nonhuman primates in which most examined neurons are strongly responsive to vestibular stimuli. This set of cortical areas thus has been labeled the "inner circle of the vestibular cortex" and is indicated in Figure 1 [Guldin et al., 1992; Guldin and Grusser, 1998; for a review see Brandt and Dieterich, 1999]. This network includes area 2v at the tip of the intraparietal sulcus, area 3aV (the neck, trunk, and vestibular region of area 3a), frontal area 6 and area 7 in the inferior parietal lobule of these animals (Fig. 1). However, the cortical area, which is interconnected most densely with all other "vestibular" areas and with the vestibular brainstem, is the parieto-insular vestibular cortex (PIVC) in the depth of the Sylvian fissure [Akbarian et al., 1988; Grusser et al., 1990a,b; Guldin and Grusser, 1998]. This area is located in the posterior parietal operculum/retroinsular region, extending into the posterior parts of the insular lobe.

Evidence for the existence of a human analogue to PIVC at a similar location as described for nonhuman primates has been provided by lesion studies of stroke patients suffering from vestibular syndromes such as unsteadiness of gait [Cereda et al., 2002], nystagmus [Takeda et al., 1995], vertigo [Brandt et al., 1995; Debette et al., 2003] or spatial hemineglect [Brandt and Dieterich, 1999]. In most of these patients, symptoms were caused by lesions in the posterior insular and adjacent parietal cortex. Such lesions are thus consistent with the anatomic location of the PIVC in nonhuman primates. In agreement with clinical observations, activations of the posterior parietal operculum/the posterior insular have been described in functional neuroimaging studies using caloric [Bottini et al., 1994, 2001; Deutschlander et al., 2002; Fasold et al., 2002; Naito et al., 2003] and galvanic vestibular stimulation [GVS; Bense et al., 2001; Fink et al., 2003; Lobel et al., 1998, 1999]. There is thus plenty of evidence that a human equivalent of PIVC may exist in the human posterior parietal operculum, probably encroaching onto the retroinsular or insular cortex. However, the exact anatomic characterization of this area in combination with functional data remains lacking.

In a recent anatomic brain mapping study, we examined the cytoarchitectonic organization of the human parietal operculum and demonstrated four distinct cortical areas within this region, OP 1–4 [Fig. 2; Eickhoff et al., 2005c]. Three of these areas seem to be equivalent to the subregions of the secondary somatosensory cortex (SII) in nonhuman primates [review by Kaas and Collins, 2003], based on their topology and a meta-analysis of functional imaging studies [Eickhoff et al., 2005a]. More precisely, area OP 1 was suggested to be equivalent to primate area SII, area OP 4 to the primate parietal ventral area PV, and OP 3 to the ventral somatosensory area VS in nonhuman primates. No equivalent could be ascertained for area OP 2, which is located deep within the Sylvian fissure at the junction of the posterior parietal operculum with the insular/retroinsular region. We test the hypothesis that area OP 2 might be the human equivalent of PIVC by reanalyzing a functional magnetic resonance imaging (fMRI) experiment that used galvanic vestibular nerve stimulation to activate the vestibular cortex [Fink et al., 2003] and examining the location of the resulting activations with respect to the probabilistic map of OP 2.

## MATERIALS AND METHODS

The methods of the functional imaging study have been reported in detail previously [Fink et al., 2003]. We summarize here the main aspects of this study.

### Subjects and Stimulation

Eleven healthy, right-handed, male volunteers (age 19–36 years, mean age 26.6 ± 5.8 years) with no history of neurologic, psychiatric, or vestibular illness gave informed consent. The study was approved by the ethics committee of the RWTH Aachen, Germany. GVS was applied via adhesive carbon electrodes placed over both mastoid processes. The polarity of the applied electric currents could be changed to allow stimulation with the anode on the subjects' left and the cathode on the subjects' right mastoid (condition LR) or in reversed polarity (cathode on the left, anode on the right; condition RL). It is well known that the effects of galvanic stimulation depend on the exact position of the electrode, the body position (upright or supine), and the skin resistance. These effects can be quite variable; therefore, we adjusted the current's power during galvanic stimulation for each subject according to the subjective (perceived tilt) and objective (nystagmus) vestibular effects elicited. This was carried out just before fMRI data acquisition, while the subject was already positioned on the scanner table. The individual current levels were 2 mA, n = 2; 2.5 mA, n = 9; and 3 mA, n = 1 [see Fink et al., 2003 for more details].

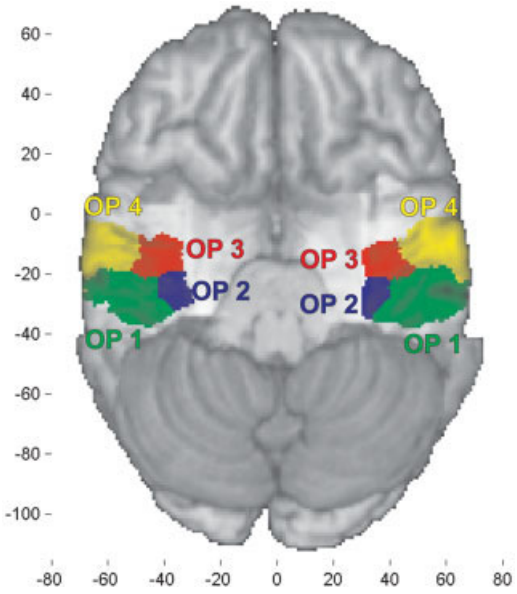


**Figure 2.**
The cytoarchitectonic organization of the human parietal operculum, shown as a maximum probability map (MPM) projected onto a surface rendering of the Montreal Neurological Institute (MNI) single-subject template. The temporal lobes were removed for display purposes. Four distinct architectonic areas can be identified in this region: OP 1–4 [Eickhoff et al., 2005c].

The fMRI paradigm consisted of four sessions, each of which started with a baseline of 24 s (6 × repetition time [TR]) followed by 12 repetitions of a cycle with a 24-s (6 × TR) activation period and a 24-s (6 × TR) baseline period. The order of the experimental conditions was pseudorandomized between sessions and subjects. During one-third of the stimulation periods, subjects had to simultaneously perform a line bisection judgment. The activations related to task performance and the interaction between task performance and GVS are described in detail elsewhere [Fink et al., 2003].

### fMRI Procedure and Image Preprocessing

Functional MR images were acquired on a 1.5 T whole-body scanner (Siemens Vision; Siemens, Erlagen, Germany) with a gradient-echo echo-planar imaging (EPI) pulse sequence (echo time [TE] = 66 ms, TR = 4 s, flip angle = 90 degrees, slice thickness = 4.00 mm, interslice gap = 0.4 mm, field of view [FOV] = 200 mm, and in-plane resolution = 3.125 × 3.125 mm) using blood oxygenation level-dependent (BOLD) contrast. Thirty slices were obtained for whole-brain coverage, oriented in the plane of the anterior–posterior commissure (AC–PC). Additional high-resolution anatomic images were acquired using a T1-weighted 3D magnetization prepared rapid acquisition gradient echo (MP-RAGE) sequence (TE = 4.4 ms, TR = 11.4 ms, flip angle = 15 degrees, inversion time [TI] = 300 ms, matrix = 200 × 256, FOV = 20 cm, 128 sagittal slices, and slice thickness = 1.25 mm).

For the purpose of the current study, the images were reanalyzed on a Pentium 4 Windows XP system using statistical parametric mapping (*SPM2*; online at http://www.fil.ion.ucl.ac.uk/spm). To allow for steady-state magnetization, the first four scans in each session were discarded. The remaining images were corrected for head movement between scans by an affine registration [Ashburner and Friston, 2003b]. The high-resolution anatomic scan was coregistered to the mean of the realigned (functional) images and then spatially normalized to the T1-weighted Montreal Neurological Institute (MNI single-subject template [Collins et al., 1994; Evans et al., 1992; Holmes et al., 1998] using linear

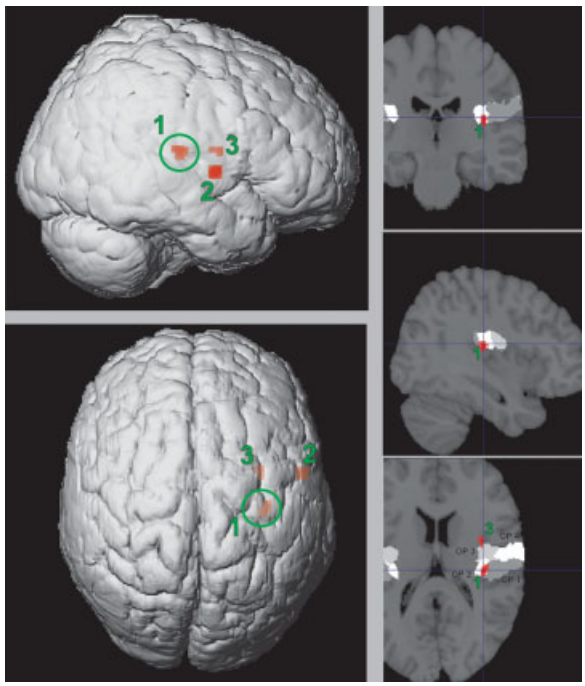


**Figure 3.**
Left panel: Relative increases in blood oxygenation level-dependent (BOLD) signal (for the 11 subjects) associated with the excitation of the right and inhibition of the left vestibular nerve (i.e., left anodal to right cathodal galvanic vestibular stimulation, condition LR) relative to rest. Areas of significant relative increase in BOLD signal ($P < 0.00005$, uncorrected) are shown superimposed on a surface-rendered Montreal Neurological Institute (MNI) single-subject template to detail the macroanatomic location of the activations. The exact coordinates and the height of the local maxima within the areas of activation as well as quantitative descriptions (probabilities) of their cytoarchitectonic assignments are given in Table I. The green numbers in the figure point to the respective cluster label in Table I. Right panel: Orthogonal sections at $x = 38$, $y = -26$, $z = 20$, i.e., the location of the local maximum of the cluster centered upon the right posterior parietal operculum (Cluster 1) corresponding to parieto-insular vestibular cortex (PIVC). The extent of OP 1 (white), OP 2 (dark gray), OP 3 (light gray), and OP 4 (intermediate gray) is shown in different gray values superimposed on the MNI single-subject template.

proportions and a nonlinear sampling algorithm [Ashburner and Friston, 2003a,c]. The resulting normalization parameters were subsequently applied to the EPI volumes, which were hereby transformed into standard stereotaxic space and resampled at 2 × 2 × 2 mm voxel size. These normalized functional images were spatially smoothed using an 8-mm full-width at half-maximum (FWHM) Gaussian kernel to meet the statistical requirements of the general linear model and to compensate for residual anatomic variation across subjects.

### Statistical Analysis

Data were analyzed in the context of the general linear model employed by *SPM2*. For each subject, we defined a design matrix modeling the experimental conditions using a boxcar reference vector convolved with a canonical hemodynamic response function (HRF) modeling the delayed BOLD response after onset of the galvanic stimulation. Subject-specific low-frequency signal drifts were filtered using a set of discrete cosine basis functions with a cut-off period of 96 s. Temporal autocorrelations between scans were estimated using a first-order autoregressive model. Parameter estimates were subsequently calculated for each voxel using weighted least squares to provide maximum likelihood estimators based on the non-sphericity of the data [Kiebel and Holmes, 2003]. The weighting "whitens" the errors, rendering them identically and independently distributed. No global scaling was applied.

The effects of left anodal to right cathodal (LR > rest) or right anodal to left cathodal (RL > rest) were computed by applying appropriate linear contrasts. The corresponding contrast from the analysis of the individual subjects were then analyzed in a second-level analysis by one-sample *t*-test, thereby effecting a random-effects model, allowing inference to the general population [Penny and Holmes, 2003]. The resulting SPM(T) maps were then interpreted by referring to the probabilistic behavior of Gaussian random fields [Worsley et al., 1996]. Because no voxel of the whole brain passed the height threshold of $P < 0.05$ corrected for family-wise errors or false discovery rate, voxels were identified as significant only if they passed a height threshold of $T > 6.21$ ($P < 0.00005$, uncorrected) and an extend threshold of $k > 5$ voxels. Regions, which were activated by vestibular stimulation irrespective of the stimulated side, were identified by a conjunction analysis between the two analyses. To obtain only those regions, which were associated significantly with the main effect of GVS in a random-effects analysis and both individual stimulation conditions, we inclusively masked the significant effects of GVS (1/2 [LR + RL] > rest) by the results of the analyses (LR > rest) and (RL > rest) in the second-level analysis.

### Comparison With Cytoarchitectonic Data

For the comparison of the functional results with cytoarchitectonic areas, a maximum probability map (MPM) was computed that identifies the most likely anatomic area at each voxel of the MNI single-subject template [Eickhoff et al., 2005b]. This definition is based on probabilistic cytoarchitectonic maps derived from the analysis of cortical areas in a sample of 10 human postmortem brains, which were subsequently normalized to the MNI reference space. The significant results of the random-effects analysis were compared to the MPM and the complete probabilistic cytoarchitectonic maps of the individual areas of the parietal operculum in the MNI reference space using the *SPM Anatomy Toolbox* [Eickhoff et al., 2005b; see http://www.fz-juelich.de/ime/spm_anatomy_toolbox]. Finally, the group mean percent signal change of the BOLD signal within OP 2 evoked by the two modes of GVS was calculated by averaging the percent signal changes from those voxels within OP 2 that were associated most strongly with the main effect of GVS across the different subjects.

## RESULTS

### Behavioral Measures

On debriefing after the experiment, all 11 subjects reported a subjective leftward tilt of the body after left anodal to right cathodal (condition LR) and a rightward tilt after right anodal to left cathodal (condition RL) GVS. Because subjects were lying on the scanner bed in the MR scanner, a body tilt ipsiversively translates into a contralateral shift of the visual world (relative to the head). Inspection of the eye movements recorded during scanning revealed in all subjects a torsional deviation ipsiversive to the side of the anodal stimulation with a slight torsional nystagmus induced.

### Neural Activations During Left Anodal to Right Cathodal Stimulation

Excitation of the right and inhibition of the left vestibular nerve caused by left anodal to right cathodal GVS (condition LR) resulted in significant changes of the BOLD signal in the right hemisphere only. The three identified foci were located in the right subcentral gyrus, the right anterior insula, and the right posterior parietal operculum/retroinsular region (Table I, Fig. 3).

The activation on the right subcentral gyrus was located anteriorly and medially to OP 4, in the as-yet unmapped anterior part of the subcentral gyrus. It is highly unlikely that this significant cluster actually reflects an activation of area OP 4. Only 19.0% of the cluster volume was located in this area. The probability for OP 4 at the position of the local maximum was as low as 10% (10–40% for the surrounding voxel).

The local maximum of the activation centered upon the right anterior insula was found anterior to OP 3 at the most dorsal aspect of the insular lobe. Only 6.3% of the cluster volume was allocated to OP 3. Similarly, there was only a very low probability for its local maximum to be located within OP 3 (probability of 20%; 20–30% for the surrounding voxel).

The activation centered upon the posterior parietal operculum, which supposedly corresponds to the human equivalent of the PIVC, was located almost exclusively (79.5% of cluster volume) within area OP 2 (Fig. 3, right panel). The local maximum of this activation (x = +38, y = −26, z

**TABLE I. Relative increases in brain activity resulting from galvanic vestibular stimulation**

| Macroanatomic location | Cytoarchitectonic allocation (%) | Coordinates (x, y, z)[a] | *t* | Cytoarchitectonic probabilities, % (range) |
|---|---|---|---|---|
| Excitation of the right and inhibition of the left vestibular nerve[b] | | | | |
| 1. R posterior parietal operculum | OP 2: 79.5 | 38, −26, 20 | 10.14 | OP2: 70 (40–80) |
| | | | | OP1: 20 (10–40) |
| 2. R anterior subcentral gyrus | OP 4: 19 | 60, −6, 8 | 9.19 | OP 4: 10 (10–40) |
| 3. R anterior insula | None | 36, −4, −20 | 8.67 | Nil |
| Excitation of the left and inhibition of the right vestibular nerve[c] | | | | |
| 1. L parietal operculum | OP 1: 43.0 | −46, −20, 16 | 10.04 | OP1: 30 (30–40) |
| | OP 3: 14.0 | | | OP4: 20 (20–40) |
| | OP 2: 9.3 | | | OP3: 20 (10–40) |
| | OP 4: 7.0 | −38, −22, 20 | 7.16 | OP 2: 40 (30–60) |
| 2. R posterior parietal operculum | OP 2: 75 | 40, −26, 22 | 7.63 | OP 2: 80 (60–80) |
| | OP 1: 6.3 | | | |
| 3. L anterior insula | None | −42, −6, −6 | 8.67 | Nil |
| 4. L inferior parietal lobe | OP 1: 69.2 | −48, −36, 26 | 7.93 | OP 1: 30 (30–40) |

[a] All coordinates are given in anatomic Montreal Neurological Institute (MNI) space.
[b] Relative increases in brain activity resulting from left anodal/right cathodal galvanic vestibular stimulation (LR, rest), exciting the right and inhibiting the left vestibular nerve.
[c] Relative increases in brain activity resulting from right anodal/left cathodal galvanic vestibular stimulation (RL, rest), exciting the left and inhibiting the right vestibular nerve.

= +20) was assigned with a high likelihood to OP 2, as the probability for that area at this position was 70% (40–80% for the surrounding voxel). In contrast, the probability for OP 1 was only 20% (10–40%).

## Neural Activations During Right Anodal to Left Cathodal Stimulation

Right anodal to left cathodal GVS (condition RL), i.e., excitation of the left and inhibition of the right vestibular nerve, caused increased neural activity in the left anterior insular, the left inferior parietal cortex, and bilaterally in the posterior parietal operculum/retroinsular region (Table I; Fig. 4, left panel).

The activation centered upon the left anterior insular (local maximum at x = −42, y = −6, z = −6) did not match any existing probabilistic cytoarchitectonic map. It was located at the inferior-most part of the insular lobe, close to the transition to the temporal cortex.

A large part of the significant activation centered upon the inferior parietal cortex was allocated to OP 1 (69.2% of the cluster volume matched the MPM volume assigned to OP 1). However, the probability for OP 1 at the local maximum (located at x = −48, y = −36, z = +26) was only 30% (30–40%). Although parts of this activation were located within OP 1, the focus of the activation thus seemed to be located either close to or within the inferior parietal cortex, which follows OP 1 caudally and laterally [Eickhoff et al., 2005a,c; Zilles et al., 2003].

The large cluster of activation including the left parietal operculum spread into all four cytoarchitectonic areas of that region: 43.0% of its volume was located in OP 1, 14.0% in OP 3, 9.3% in OP 2, and 7.0% in OP 4. Two local maxima were identified within this cluster. One of these maxima (x = −46, y = −20, z = +16) was located at the border between OP 1 (30% probability), OP 4, and OP 3 (both 20% probability). The position of the second local maximum (x = −38, y = −22, z = +20) was assigned to OP 2 (Fig. 4, middle panel). The probability for OP 2 at this position was 40% (30–60% for the surrounding voxels). The probabilities for all other cytoarchitectonic areas at this position were <20%.

The activation observed in the right posterior parietal operculum/retroinsular region was located predominantly (75.0%) within OP 2. The local maximum within this cluster of activation (x = +40, y = −26, z = +22) was located in area OP 2 (Fig. 4, right panel). The probability for finding OP 2 at this position was 80% (60–80% for the surrounding voxels).

## Conjunction

The only brain region where a significant activation was evoked by both stimulus conditions was the posterior parietal operculum on the right hemisphere (Fig. 5A). Consequently, only this region showed a significant effect in the conjunction analysis (Fig. 5B). Only the right posterior parietal operculum thus was activated consistently by vestibular stimulation, irrespective of the stimulated side. Of this cluster's volume, 66.7% was located within OP 2; only 8.3% was allocated to OP 1. The maximum activation for the main effect of GVS was located at x = +38, y = −26, z = +22 (Fig. 5C). It was assigned with a probability of 80% to OP 2 (70–80% for the surrounding voxels), whereas the probability for OP 1 was only 20–60%.

## Percent Signal Change in OP 2

There was a consistent bilateral BOLD signal increase within area OP 2 after both left anodal to right cathodal

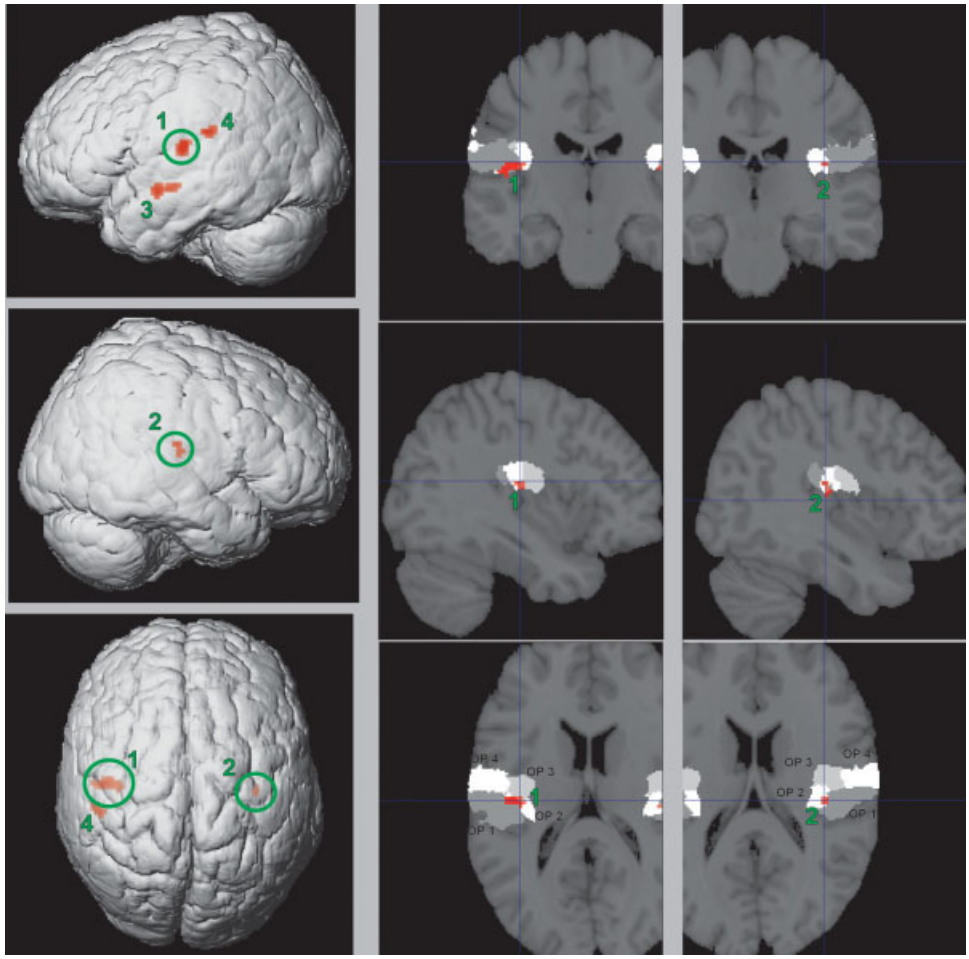


**Figure 4.**

Left panel: The regions where there is a significant relative blood oxygenation level-dependent (BOLD) signal increase associated with the excitation of the left and inhibition of the right vestibular nerve (i.e., right anodal to left cathodal galvanic vestibular stimulation, condition RL) relative to rest. Areas of significant relative increase in BOLD signal ($P < 0.00005$, uncorrected) are shown superimposed on a surface-rendered Montreal Neurological Institute (MNI) single-subject template to detail the macroanatomy. The height and the exact coordinates of the local maxima within the areas of activation as well as quantitative descriptions of their cytoarchitectonic assignments are given in Table I. The green numbers in the figure point to the respective cluster label in this table. Middle panel: Detailed view on orthogonal sections at x = −38, y = −22, z = 20, i.e., the location of the local maximum of the cluster centered upon the left posterior parietal operculum (Cluster 1) corresponding to parieto-insular vestibular cortex (PIVC). The extent of OP 1 (white), OP 2 (dark gray), OP 3 (light gray), and OP 4 (intermediate gray) is shown in different gray values; the MNI single-subject template is shown in the background. Right panel: Detail views focused on the location of the local maximum in the right posterior parietal operculum (Cluster 2, x = 40, y = −26, z = 22)

and right anodal to left cathodal stimulation (Fig. 6). The mean relative BOLD signal change after stimulation of the ipsilateral vestibular nerve was almost identical for the two hemispheres (0.35% for the left vs. 0.36% for the right hemisphere). However, the response to contralateral stimulation showed a considerable degree of lateralization into the right hemisphere. Whereas the mean percent signal change at the local maximum for condition RL in right area OP 2 was 0.30%, the respective change in the BOLD signal of the left hemisphere and condition LR, respectively, was only 0.22%. Although this effect failed to reach statistical significance ($P > 0.05$ for the interaction between area and stimulus side in a two-way analysis of variance [ANOVA]), this difference was in good accordance with the observation that only right OP 2 was activated in the conjunction of both main effects.

## DISCUSSION

We have integrated data obtained from an fMRI study using GVS and data on the cytoarchitectonic organization of the parietal operculum to identify the human equivalent of

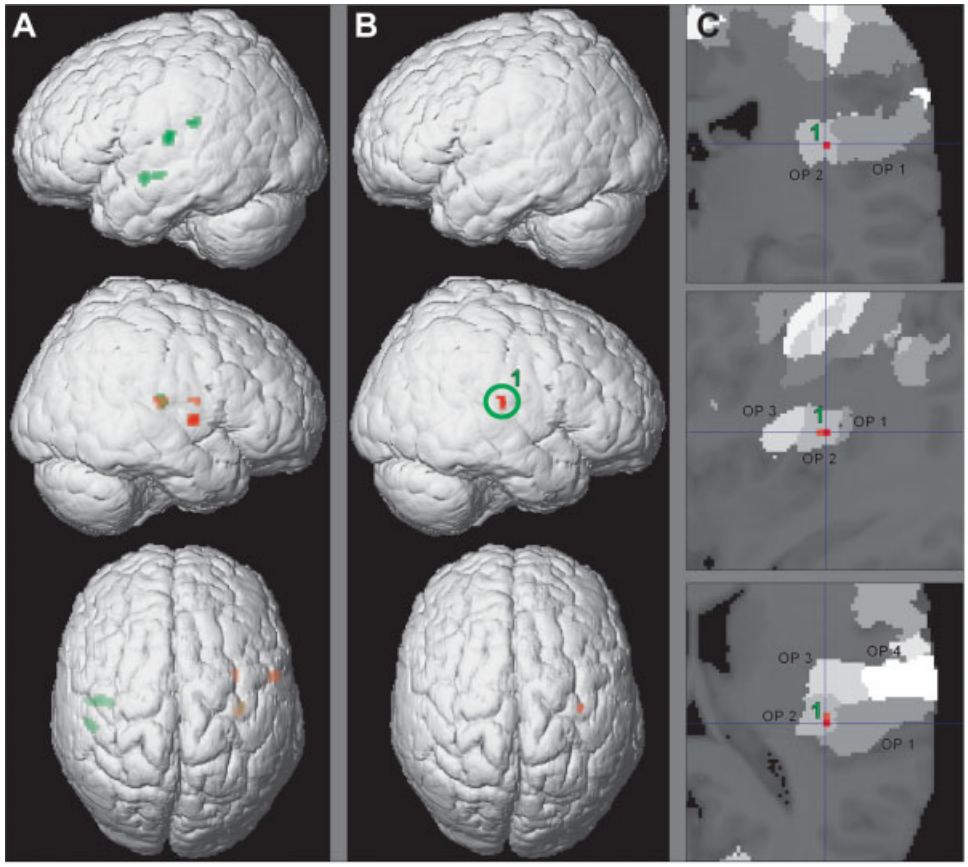


**Figure 5.**
**A:** Synopsis of the significant activations for both stimulation modes. Activations in condition RL are shown in green, those in condition LR in red. The two patterns of activation only overlap in a small region in the right hemisphere. **B:** Results of the conjunction analysis. The displayed region was significantly activated in both stimulation conditions and is associated significantly with the main effect of galvanic vestibular stimulation (irrespective of anode side) relative to rest. **C:** Orthogonal sections through the location of the local maximum revealed by the conjunction analysis, which was located in the right posterior parietal operculum (Cluster 1, x = +38, y = −26, z = +22).

the PIVC. We will now discuss the results with respect to previous findings on this area in humans and nonhuman primates.

## Vestibular Stimulation

We used GVS to activate the vestibular system. This choice was based on the several advantages of this method over caloric vestibular stimulation (CVS), in particular with respect to application in an fMRI environment. First, whereas the postural and ocular effects of CVS are mediated predominantly by the semicircular canals, with little or no otolithic component [Barany, 1907; Gentine et al., 1990], the effects of GVS are due to modulation of the tonic firing rate of *all* vestibular afferents close to their postsynaptic trigger site [Goldberg et al., 1984]. Second, the effects of CVS have a very slow time courses as the time from stimulus onset to maximal effect can take as long as 80 s and vestibular sensations can be present for as long as 15 min after stimulation [Proctor, 1988]. CVS can thus not be used efficiently in an fMRI design where activation blocks usually last around 20 s. Third, CVS provokes magnetic susceptibility artifacts due to the susceptibility difference between air and water [Lobel et al., 1998]. This may result in false-positive activations due to task correlated (artificial) changes in the MRI signal and reduces the statistical power to detect true activations due to the increased noise level.

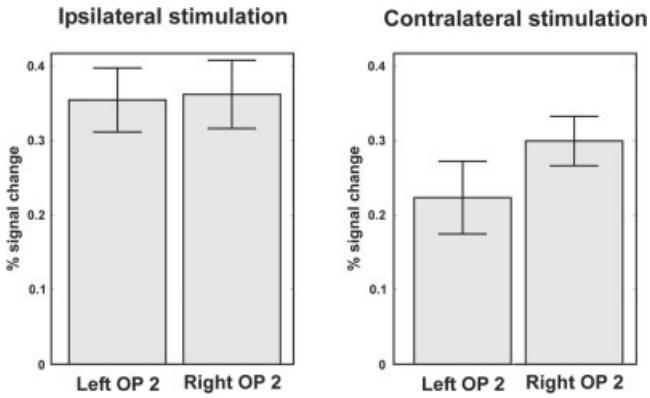


**Figure 6.**
The blood oxygenation level-dependent (BOLD) signal changes (in percent) per condition are displayed for OP 2 in both hemispheres. The values shown are the mean (± SEM) percent signal changes for the voxel within OP 2 in each subject, which was associated most strongly with the main effect of galvanic vestibular stimulation. That there is a considerable degree of lateralization into the right hemisphere for the response to contralateral stimulation, i.e., the response of right area OP 2 to excitation of the left vestibular nerve was considerably stronger than was the BOLD signal change in OP 2 of the left hemisphere caused by stimulation of the right vestibular nerve.

One potential drawback of GVS is the tactile/somatosensory component of the electrical stimulus, which might cause coactivation of the somatosensory cortices. However, in the present study we did not observe any activation in the primary somatosensory cortex after GVS, which makes a significant tactile component of our stimulation highly unlikely. Moreover, to examine if the observed activation on the parietal operculum was distinct from the secondary somatosensory cortex, the observed activation on OP 2 was compared to the functional location of the hand region within SII as defined by a meta-analysis of functional imaging studies involving tactile, thermal, kinesthetic, and electrical stimulation. Given our current knowledge of the somatotopic organization of the SII region in humans and nonhuman primates, somatosensory input from the mastoids, i.e., the locus of galvanic stimulation, should have resulted in activation lateral to the hand representation but within the same cortical areas (SII/PV, cf. the review by Kaas and Collins [2003]). However, as shown in Figure 7 the cortical response to galvanic stimulation clearly failed to follow this prediction for two reasons: (1) the functional activation after GVS was located medial and posterior to the SII hand region; and (2) GVS evoked activation in a different cortical area as compared to somatosensory paradigms.

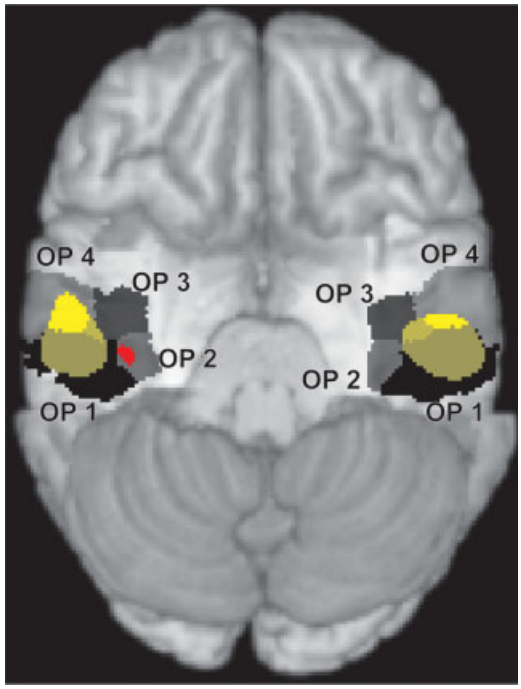


**Figure 7.**
Comparison between the location of secondary somatosensory cortex (SII) as revealed by a meta-analysis of 181 functional imaging activations [Eickhoff et al., 2005a] shown in yellow and the location of parieto-insular vestibular cortex (PIVC) identified by the conjunction analysis reported in this study, shown in red. The temporal lobes were removed for display purposes (cf. Fig. 2). Significant clusters are clearly separated from each other and are also located in different cytoarchitectonic areas: Whereas the location of SII corresponds mainly to OP 1 and OP 4, PIVC is located in area OP 2.

## Human Analogue of the PIVC

We propose that cytoarchitectonic area OP 2 constitutes the human equivalent of the PIVC as defined in nonhuman primates [Akbarian et al., 1988]. This claim is supported by homologies between OP 2 and PIVC in the functional response characteristics and the topography.

In the macaque monkey, a large proportion of the neurons in the PIVC are driven strongly by (mainly ipsilateral) input from the vestibular nuclei via the ventroposterior thalamus [Grusser et al., 1990a,b]. The PIVC is closest to the notion of a primary vestibular area, given its robust response to vestibular stimulation and its dense connections with all other vestibular areas as well as the vestibular nuclei [Akbarian et al., 1994]. Similar results were also reported for other species of nonhuman primates. All these studies show a remarkable consistency with respect to the location and response characteristics of the PIVC within the primate family [Guldin and Grusser, 1996, 1998].

Similarly, the existence of a vestibular cortex in the human parietal operculum was demonstrated repeatedly by cortical electrical stimulation [Kahane et al., 2003; Penfield and Jasper, 1954] and functional imaging studies using vestibular stimulation [Bense et al., 2001; Bottini et al., 1994, 2001; Deutschlander et al., 2002; Fasold et al., 2002; Fink et al., 2003; Lobel et al., 1998, 1999] or head movements [Petit and Beauchamp, 2003]. These observations led to the conclusion that an equivalent to the primate area PIVC also exists in the human brain and that it is located at a comparable position in the posterior parietal operculum [Brandt and Dieterich, 1999]. We were able to replicate the above findings by demonstrating bilaterally significant increased BOLD signals in the deep posterior parietal operculum after GVS.

For the first time, the anatomic substrate of these cortical vestibular activations could now be identified by correlating these functional imaging results with cytoarchitectonic data of the human parietal operculum. When the probabilistic cytoarchitectonic maps for the opercular areas OP 1–4 were compared to the location of the functional activations of the parietal operculum elicited by GVS, a very good correspondence could be demonstrated between these activations and the extent of area OP 2. Importantly, the match between OP 2 and the vestibular activation was much better than was the match between this activation and any other architectonic area within the parietal operculum, based on the number of overlapping voxels and the probabilities for different cytoarchitectonic areas at the location of the local maxima of the activation. This specific activation of OP 2 by GVS, which was used repeatedly to functionally demonstrate the existence of a human PIVC as described above, provides strong evidence for our hypothesis that cytoarchitectonic area OP 2

is the structural analogue in the human cerebral cortex to the PIVC of nonhuman primates.

This hypothesis is supported further by similarities in the topology between PIVC and OP 2. In the cortex of nonhuman primates, PIVC is located medially in the posterior parietal operculum, close to or within the circular sulcus of the insula. It is followed rostrally and to some extent also laterally by the secondary somatosensory cortex [Akbarian et al., 1988; Grusser et al., 1990a], which in turn consists of three anatomically and functionally distinct areas [Kaas and Collins, 2003]. The topography of human area OP 2 is in good agreement with the location of PIVC in nonhuman primates. OP 2 is located medially on the posterior parietal operculum, reaching into the retroinsular region. Similar to area PIVC in monkeys, it is mainly found close to the circular sulcus of the insular. Area OP 2 is followed rostrally and laterally by areas OP 1, OP 3, and OP 4. These areas show a very good topographic match to the areas SII (OP 1), the parietal ventral (PV) area (OP 4), and the ventral somatosensory area VS (OP 3) of the primate SII complex [Eickhoff et al., 2005a,c; Kaas and Collins, 2003] and may thus be considered to constitute the human equivalents of these areas [Young et al., 2004]. This supposed correspondence is in good accordance with the results of a recent meta-analysis of the locations of SII activations in functional imaging studies [Eickhoff et al., 2005a], which confirmed that the coordinates of the functional locations of SII correspond closely to OP 1 and OP 4, i.e., primate areas SII and PV (Fig. 7). The location of area PIVC, as functionally identified in this study, is clearly separated from the location of SII as revealed by that meta-analysis, in terms of stereotaxic coordinates and its underlying cytoarchitectonic areas.

Interestingly, the cytoarchitecture of OP 2 also points toward the interpretation of OP 2 as a primary sensory area, because OP 2 differs distinctly from the surrounding cortex by showing a relatively wide and cell dense inner granular layer IV (Fig. 8) while lacking prominent pyramidal cells (in layers III and V). This koniocortical cytoarchitecture resembles the architecture of other primary sensory areas, e.g., area 3b in the somatosensory system [Geyer et al., 1999], area 41 in the auditory system [Morosan et al., 2001], and most pronounced area 17 of the visual system [Amunts et al., 2000]. However, the koniocortical features in OP 2 are not as prominent as in the other primary cortices. This might relate to electrophysiologic observations made in the macaque monkey, that the PIVC is not a strictly unimodal vestibular area but also shows responses to visual and somatosensory stimuli [Akbarian et al., 1988; Grusser et al., 1990a,b; Guldin and Grusser, 1998]. These polymodal response characteristics distinguish PIVC (i.e., OP 2) from unimodal primary sensory areas like 3b, 41, and 17, and might be reflected in the less-distinct koniocortical architecture of OP 2.

Our current results contradict the earlier notion suggesting that the posterior insular is human PIVC [cf. Brandt and Dieterich, 1999; Dieterich et al., 1998; Emri et al., 2003; Indovina et al., 2005]. The demonstrated lack of activation of the posterior insular in a situation that should have activated

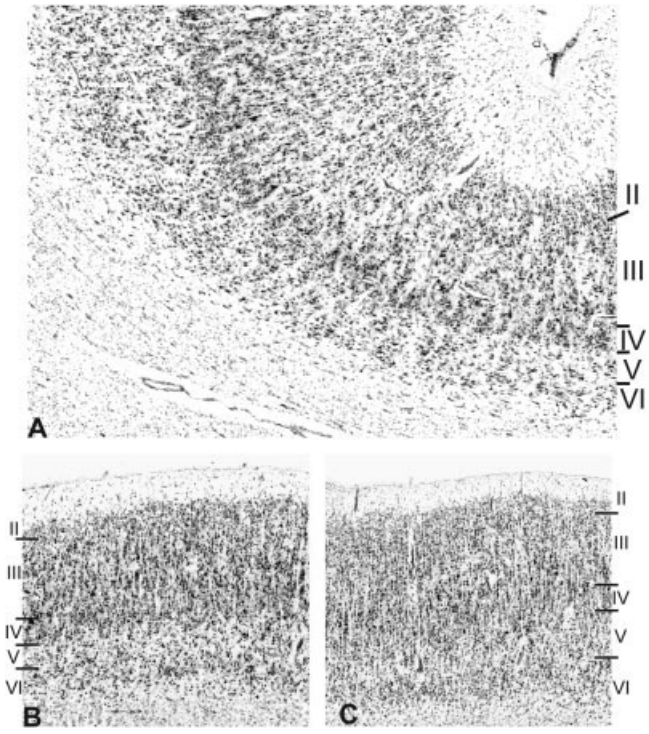


**Figure 8.**

A) Microphotograph of area OP 2 from a cell body-stained histological section. The thin cortex of OP 2 shows small infragranular layers, a sharply defined white matter border, and a distinct horizontal lamination. Prominent pyramidal cells in layer III are rare. The cytoarchitecture of OP 2 is more similar to that of Brodmann area (BA) 3b (**B**), i.e., the primary somatosensory cortex, than to the unimodal somatosensory association area BA 1 (**C**). Roman numbers designate cortical layers.

PIVC is supported by other observations that locate PIVC not in the insular cortex but on the parietal operculum [e.g., Fasold et al., 2002; Lobel et al., 1999; Petit and Beauchamp, 2003]. This view is also in line with results from direct cortical stimulation of the insular cortex, which rarely elicits vestibular reactions [Kahane et al., 2003; Ostrowsky et al., 2002; Penfield and Jasper, 1954].

In this context, it is important to keep in mind, that OP 2 often also extends onto the upper part of the insular lobe, i.e., behind the circular sulcus of the insula [Eickhoff et al., 2005a,b]. Nevertheless, this area can be classified unambiguously as a parietal opercular area due to its main location on the upper bank of the Sylvian fissure and its architectonic distinction from the insular cortex. Given our current results, it thus seems that vestibular activations reported previously as being located on posterior insular should rather be attributed to area OP 2. This controversy highlights the great benefit of using microstructural data as the anatomic reference for the localization of functional imaging results instead of macroanatomic descriptions: Only by comparison with (cyto-) architectonic data in the same reference space does it become possible to reliably infer the anatomic loca-

tion of a functional activation and accordingly provide correct structural labels.

### Hemispheric Asymmetry

The effects observed during left and right anodal GVS, respectively, show differential patterns of hemispheric activation: inhibition of the left and excitation of the right vestibular nerve (condition LR) resulted in significant activation of OP 2 (i.e. PIVC) in the right hemisphere. whereas inhibition of the right and excitation of the left vestibular nerve (condition RL) bilaterally evoked significant activation in OP 2. This suggests right hemispheric dominance for the processing of vestibular information (in the sense that both right and left vestibular nerve stimulation activate the right hemisphere). This view is corroborated by the conjunction analysis, which showed, that only OP 2 on the right hemisphere was activated by GVS regardless of polarity. This hemispheric asymmetry of vestibular processing is in good accordance with the results of previous functional imaging studies [Bense et al., 2001; Dieterich et al., 1998, 2003; Fasold et al., 2002; Suzuki et al., 2001; but see Bottini et al., 1994].

OP 2 does not show any architectonic asymmetry [Eickhoff et al., 2005a,c]. Neither the cytoarchitectonic pattern nor the stereotaxic location or the cortical volumes of this area were significantly different between the hemispheres. The observed functional asymmetry may thus originate from differences in connectivity, resulting in different amounts of afferent input into these areas. In principle, this different input may be mediated via transcallosal connections from left OP 2 to its right hemispheric counterpart, or may result from differently weighted subcortical inputs. This issue has to be addressed in further experiments.

## CONCLUSION

We have been able to identify area OP 2 as the human equivalent of the primate PIVC by combining functional imaging and probabilistic cytoarchitectonic mapping. PIVC plays a unique role in the vestibular cortex due to its robust response to vestibular stimuli and its dense connections with cortical and subcortical vestibular structures. Our functional data (as previous data) suggest a right hemisphere dominance for vestibular processing, an effect that is not mirrored by cytoarchitectonic asymmetries in OP 2, the anatomic equivalent of PIVC. Further investigations of the cortical vestibular network will be necessary to gain a better understanding of its organization and its interactions with other cortical systems, e.g., the mechanisms underlying spatial orientation and attention, body posture, or gaze. However, the architectonic identification of the human equivalent of area PIVC, which is a key area of system, is one important step toward this goal.

## ACKNOWLEDGMENTS

We thank Dr. Thomas Stephan and Prof. Marianne Dieterich for their help with the original fMRI study.

## REFERENCES

Akbarian S, Berndl K, Grusser OJ, Guldin W, Pause M, Schreiter U (1988): Responses of single neurons in the parietoinsular vestibular cortex of primates. Ann N Y Acad Sci 545:187–202.

Akbarian S, Grusser OJ, Guldin WO (1994): Corticofugal connections between the cerebral cortex and brainstem vestibular nuclei in the macaque monkey. J Comp Neurol 339:421–437.

Amunts K, Malikovic A, Mohlberg H, Schormann T, Zilles K (2000): Brodmann's areas 17 and 18 brought into stereotaxic space—where and how variable? Neuroimage 11:66–84.

Ashburner J, Friston KJ (2003a): High-dimensional image warping. In: Zeki S, Ashburner JT, Penny WD, Frackowiak RSJ, Friston KJ, Frith CD, Dolan RJ, Price CJ, editors. Human brain function. Oxford: Academic Press. p 673–694.

Ashburner J, Friston KJ (2003b): Rigid body registration. In: Zeki S, Ashburner JT, Penny WD, Frackowiak RSJ, Friston KJ, Frith CD, Dolan RJ, Price CJ, editors. Human brain function. Oxford: Academic Press. p 635–653.

Ashburner J, Friston KJ (2003c): Spatial normalization using basis functions. In: Zeki S, Ashburner JT, Penny WD, Frackowiak RSJ, Friston KJ, Frith CD, Dolan RJ, Price CJ, editors. Human brain function. Oxford: Academic Press. p 655–672.

Barany R (1907): New methods of examination of the semicircular canals and their practical significance. Ann Ophtalmol 16:755–861.

Bense S, Stephan T, Yousry TA, Brandt T, Dieterich M (2001): Multisensory cortical signal increases and decreases during vestibular galvanic stimulation (fMRI). J Neurophysiol 85: 886–899.

Berthoz A (1996): How does the cerebral cortex process and utilize vestibular signals. In: Baloh RW, Halmagyi GM, editors. Disorders of the vestibular system. Oxford: Oxford University Press. p 113–125.

Bottini G, Karnath HO, Vallar G, Sterzi R, Frith CD, Frackowiak RS, Paulesu E (2001): Cerebral representations for egocentric space: Functional-anatomical evidence from caloric vestibular stimulation and neck vibration. Brain 124:1182–1196.

Bottini G, Sterzi R, Paulesu E, Vallar G, Cappa SF, Erminio F, Passingham RE, Frith CD (1994): Identification of the central vestibular projections in man: a positron emission tomography activation study. Exp Brain Res 99:164–169.

Brandt T, Bötzel K, Yousry TA, Dieterich M, Schulze S (1995): Rotational vertigo in embolic stroke of the vestibular and auditory cortices. Neurology 45:42–44.

Brandt T, Dieterich M (1999): The vestibular cortex. Its locations, functions, and disorders. Ann N Y Acad Sci 871:293–312.

Cereda C, Ghika J, Maeder P, Bogousslavsky J (2002): Strokes restricted to the insular cortex. Neurology 59:1950–1955.

Collins DL, Neelin P, Peters TM, Evans AC (1994): Automatic 3D intersubject registration of MR volumetric data in standardized Talairach space. J Comput Assist Tomogr 18:192–205.

Debette S, Michelin E, Henon H, Leys D (2003): Transient rotational vertigo as the initial symptom of a middle cerebral artery territory infarct involving the insula. Cerebrovasc Dis 16:97–98.

Deutschlander A, Bense S, Stephan T, Schwaiger M, Brandt T, Dieterich M (2002): Sensory system interactions during simultaneous vestibular and visual stimulation in PET. Hum Brain Mapp 16:92–103.

Dieterich M, Bense S, Lutz S, Drzezga A, Stephan T, Bartenstein P, Brandt T (2003): Dominance for vestibular cortical function in the non-dominant hemisphere. Cereb Cortex 13:994–1007.

Dieterich M, Bucher SF, Seelos KC, Brandt T (1998): Horizontal or vertical optokinetic stimulation activates visual motion-sensitive, ocular motor and vestibular cortex areas with right hemispheric dominance. An fMRI study. Brain 121:1479–1495.

Eickhoff SB, Amunts K, Mohlberg H, Zilles K (2005a): The human parietal operculum: II. Stereotaxic maps and correlation with functional imaging results. Cereb Cortex in press.

Eickhoff SB, Stephan KE, Mohlberg H, Grefkes C, Fink GR, Amunts K, Zilles K (2005b): A new SPM toolbox for combining probabilistic cytoarchitectonic maps and functional imaging data. Neuroimage 25:1325–1335.

Eickhoff SB, Zilles K, Schleicher A, Amunts K (2005c): The human parietal operculum: I. Cytoarchitectonic mapping of subdivisions. Cereb Cortex in press.

Emri M, Kisely M, Lengyel Z, Balkay L, Marian T, Miko L, Berenyi E, Sziklai I, Tron L, Toth A (2003): Cortical projection of peripheral vestibular signaling. J Neurophysiol 89:2639–2646.

Evans AC, Marrett S, Neelin P, Collins L, Worsley K, Dai W, Milot S, Meyer E, Bub D (1992): Anatomical mapping of functional activation in stereotaxic coordinate space. Neuroimage 1:43–53.

Fasold O, von Brevern M, Kuhberg M, Ploner CJ, Villringer A, Lempert T, Wenzel R (2002): Human vestibular cortex as identified with caloric stimulation in functional magnetic resonance imaging. Neuroimage 17:1384–1393.

Fink GR, Marshall JC, Weiss PH, Stephan T, Grefkes C, Shah NJ, Zilles K, Dieterich M (2003): Performing allocentric visuospatial judgments with induced distortion of the egocentric reference frame: an fMRI study with clinical implications. Neuroimage 20:1505–1517.

Fredrickson JM, Figge U, Scheid P, Kornhuber HH (1966): Vestibular nerve projection to the cerebral cortex of the rhesus monkey. Exp Brain Res 2:318–327.

Gentine A, Eichhorn JL, Kopp C, Conraux C (1990): Modelling the action of caloric stimulation of the vestibule. I. The hydrostatic model. Acta Otolaryngol 110:328–333.

Geyer S, Schleicher A, Zilles K (1999): Areas 3a, 3b, and 1 of human primary somatosensory cortex: 1. Microstructural organization and interindividual variability. Neuroimage 10:63–83.

Goldberg JM, Smith CE, Fernandez C (1984): Relation between discharge regularity and responses to externally applied galvanic currents in vestibular nerve afferents of squirrel monkey. J Neurophysiol 5:1236–1256.

Grusser OJ, Pause M, Schreiter U (1990a): Localization and responses of neurones in the parieto-insular vestibular cortex of awake monkeys (*Maccaca fascicularis*). J Physiol 430:537–557.

Grusser OJ, Pause M, Schreiter U (1990b): Vestibular neurones in the parieto-insular cortex of monkeys (*Maccaca fascicularis*): visual and neck receptor responses. J Physiol 430:559–583.

Guldin W, Grusser OJ. 1996. The anatomy of vestibular cortices in of primates. In: Collard, Jeannerod, Christen.Y, editors. Le Cortex Vestibulaire. Boulogne: Ipsen. p 17–26

Guldin WO, Akbarian S, Grusser OJ (1992): Cortico-cortical connections and cytoarchitectonics of the primate vestibular cortex: a study in squirrel monkeys (*Saimiri sciureus*). J Comp Neurol 326:375–401.

Guldin WO, Grusser OJ (1998): Is there a vestibular cortex? Trends Neurosci 21:254–259.

Holmes CJ, Hoge R, Collins L, Woods R, Toga AW, Evans AC (1998): Enhancement of MR images using registration for signal averaging. J Comput Assist Tomogr 22:324–333.

Indovina I, Maffei V, Bosco G, Zago M, Macaluso E, Lacquaniti F (2005): Representation of visual gravitational motion in the human vestibular cortex. Science 308:416–419.

Kaas JH, Collins CE (2003): The organization of somatosensory cortex in anthropoid primates. Adv Neurol 93:57–67.

Kahane P, Hoffmann D, Minotti L, Berthoz A (2003): Reappraisal of the human vestibular cortex by cortical electrical stimulation study. Ann Neurol 54:615–624.

Kiebel S, Holmes AP (2003): The general linear model. In: Zeki S, Ashburner JT, Penny WD, Frackowiak RSJ, Friston KJ, Frith CD, Dolan RJ, Price CJ, editors. Human brain function. Oxford: Academic Press. p 725–760.

Lobel E, Kleine JF, Bihan DL, Leroy-Willig A, Berthoz A (1998): Functional MRI of galvanic vestibular stimulation. J Neurophysiol 80:2699–2709.

Lobel E, Kleine JF, Leroy-Willig A, Van de Moortele PF, Le Bihan D, Grusser OJ, Berthoz A (1999): Cortical areas activated by bilateral galvanic vestibular stimulation. Ann N Y Acad Sci 871:313–323.

Morosan P, Rademacher J, Schleicher A, Amunts K, Schormann T, Zilles K (2001): Human primary auditory cortex: cytoarchitectonic subdivisions and mapping into a spatial reference system. Neuroimage 13:684–701.

Naito Y, Tateya I, Hirano S, Inoue M, Funabiki K, Toyoda H, Ueno M, Ishizu K, Nagahama Y, Fukuyama H, Ito J (2003): Cortical correlates of vestibulo-ocular reflex modulation: a PET study. Brain 126:1562–1578.

Ödkvist LM, Rubin AM, Schwarz DWF, Fredrickson JM (1973): Vestibular and auditory cortical projection in the guinea pig (*Cavia porcellus*). Exp Brain Res 18:279–286.

Ostrowsky K, Magnin M, Ryvlin P, Isnard J, Guenot M, Mauguiere F (2002): Representation of pain and somatic sensation in the human insula: a study of responses to direct electrical cortical stimulation. Cereb Cortex 12:376–385.

Penfield W, Jasper H (1954): Epilepsy and functional anatomy of the human brain. Boston, Ma: Little, Brown & Co.

Penny WD, Holmes AP (2003): Random effects analysis. In: Zeki S, Ashburner JT, Penny WD, Frackowiak RSJ, Friston KJ, Frith CD, Dolan RJ, Price CJ, editors. Human brain function. Oxford: Academic Press. p 843–850.

Petit L, Beauchamp MS (2003): Neural basis of visually guided head movements studied with fMRI. J Neurophysiol 89:2516–2527.

Proctor LR (1988): Clinical experience with a short-acting, adjustable caloric stimulation. In: Vestibular Disorders. Barber HO, Sharpe JA, editors. Chicago: Yearbook Medical Publishers. p 87–96.

Suzuki M, Kitano H, Ito R, Kitanishi T, Yazawa Y, Ogawa T, Shiino A, Kitajima K (2001): Cortical and subcortical vestibular response to caloric stimulation detected by functional magnetic resonance imaging. Brain Res Cogn Brain Res 12:441–449.

Takeda N, Tanaka-Tsuji M, Sawada T, Koizuka I, Kubo T (1995): Clinical investigation of the vestibular cortex. Acta Otolaryngol Suppl 520:110–112.

Vogeley K, Fink GR (2003): Neural correlates of the first-person-perspective. Trends Cogn Sci 7:38–42.

Worsley KJ, Marrett S, Neelin P, Vandal AC, Friston KJ, Evans AC (1996): A unified statistical approach for determining significant signals in images of cerebral activation. Hum Brain Mapp 4:58–74.

Young JP, Herath P, Eickhoff S, Choi J, Grefkes C, Zilles K, Roland PE (2004): Somatotopy and attentional modulation of the human parietal and opercular regions. J Neurosci 24:5391–5399.

Zilles K, Eickhoff S, Palomero-Gallagher N (2003): The human parietal cortex: a novel approach to its architectonic mapping. Adv Neurol 93:1–21.